

EXPLORATION OF QUENCH INITIATION DUE TO INTENTIONAL GEOMETRICAL DEFECTS IN A HIGH MAGNETIC FIELD REGION OF AN SRF CAVITY*

J.Dai[#], A.D.Palczewski, G.Eremeev, R.L.Geng, TJNAF, Newport News, VA 23606, USA
 K.Zhao, Institute of Heavy Ion Physics, Peking University, Beijing 100871, China

Abstract

A CEBAF shape single cell cavity with four intentional geometrical defects was built at Jefferson lab to research the influence of magnetic field enhancement on the quench initiation of SRF cavity. This cavity has been RF tested with the T-mapping system at Jefferson lab. Experimental result shows that quench location appears at one of the four intentional geometrical defects and preheating phenomenon occurs at all four intentional defects. At all other areas of the cavity, except the four intentional defects, almost no preheating is found. The fabrication procedures and the surface characterization of the four defects, the preheating phenomenon and associated quench initiation analysis of this cavity are presented here.

INTRODUCTION

Recent RF tests and surface morphology for a few of nine-cell SRF cavities at Jefferson lab (TB9RI019, PKU2, TB9NR001) show that there are always some geometrical defects near each quench site. The quench location and associated preheating data of these cavities were obtained by T-mapping and OST (Oscillating Superleak Transducers) technique [1-3]. Subsequently, optical inspection of these defects was performed by a high-resolution optical inspection machine (“Kyoto camera” [4]). The inspection shows that most of the defects have the same topographical structure [5]. Further analysis indicates that this kind of topographical structure has a pit-type shape. Subsequently, replica-profilometry technique [6, 7] was used to characterize the profile details of these defects; it also indicates that most of the defects are pit type shape, see the examples in Figure 1.

The quench sites in these 9-cell cavities are all at the EBW (electron beam welding) area, where the magnetic field is highest. We assume the magnetic field enhancement of the pit-like defects would contribute to the quench initiation. In order to verify this assumption, one CEBAF style single cell cavity with four intentional geometrical defects was fabricated to research the influence of magnetic field enhancement on the preheating and quench phenomenon in SRF cavities. The experiment results and some preliminary analysis of preheating data are presented here.

*Authored by Jefferson Science Associates, LLC under U.S. DOE Contract No. DE-AC05-06OR23177

[#]daijin@pku.edu.cn

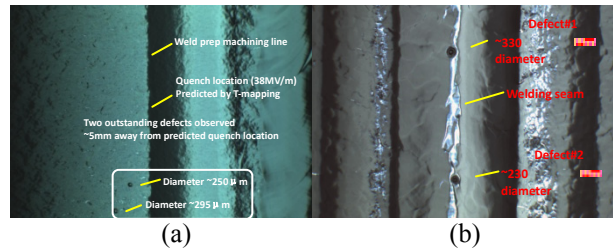


Figure 1: Defect examples near quench location: (a) nine-cell cavity TB9RI019, two pit-type defects observed ~5mm away from the predicted quench location; (b) nine-cell cavity TB9NR001, two pit-type defects were found near the quench site.

DEFECT FABRICATION

The initial fabrication goal was to make four pits in the cavity without introducing any foreign material. This would ensure the geometrical shape and associated magnetic field enhancement would play the leading role to the RF performance.

The four pits were chosen to be located near the equator area where the magnetic field is highest. The pits were machined by a TRAK DPM3 CNC Mill with a 400 μm diameter diamond drill (HOO micron ball end mill), as shown in Figure 2.

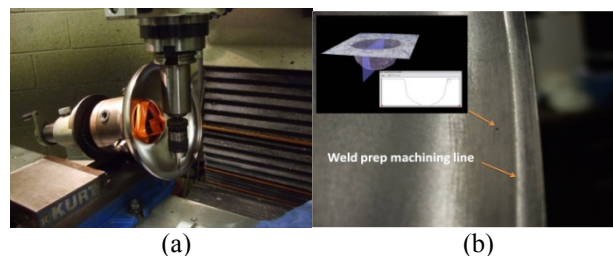


Figure 2: (a) The fabrication of pit-kind geometrical defect; (b) One intentional pit-kind defect on the fabricated cavity.

The cavity was mounted on a holder with rubber foot to protect cavity inner surface. The angle between the axis of cavity and the ground was 13° to allow the drill to be perpendicular to the cavity equator area. The velocity of the mill was set at 5000 RPM when the four pit-type defects were fabricated. After mechanical fabrication, some sharp bumps were found at the rim of each pit. Mechanical polishing was performed to remove this kind of sharp edge for each pit by a grind paper. Subsequently, 10 μm BCP was performed to clean the cavity for equator welding. After welding, an additional 5 μm BCP was performed for RF test preparation. The total 15 μm BCP is

expected to attain a 10~20 μm curvature radius at the edge of each pit. This means the magnetic field enhancement factor for each pit is about 3 (ANSYS simulation, see Table 1 & 2).

Note: there are four critical geometrical parameters for pit-type defect:

- (1) R: the diameter of the pit.
- (2) L: the depth of the pit.
- (3) r: the curvature radius of the rim of the pit.
- (4) dz: the distance between defect and under-bead center of cavity.

Table1: ANSYS simulation for field enhancement factor of six kinds of pit-type defect

Pit type	R/μm	L/μm	r/μm	β
1	500	800	10	3.35
2	500	800	20	2.70
3	500	800	30	2.38
4	500	250	10	3.26
5	500	250	20	2.64
6	500	250	30	2.34

Table 2: The designed geometrical parameters of 4 pits in cavity C1-3

Pit #	R/μm	L/μm	dz/mm	r/μm	β
1	500	800	6.0	10~20	2.7~3.3
2	500	800	9.0	10~20	2.7~3.3
3	500	250	6.0	10~20	2.6~3.2
4	500	250	9.0	10~20	2.6~3.2

If we assume the critical magnetic field at 2K is 200mT, for this cavity, $\frac{B_p}{E_{acc}} = 4.43$, it means the applied

magnetic field on this cavity will exceed its critical magnetic field at the gradient about 10~15MV/m.

GEOMETRICAL CHARACTERIZATION AND FOREIGN MATERIAL INSPECTION

Pilot sample preparation

Once the cavity is welded, it's inconvenient to observe its inner condition. In order to research the geometrical and chemical characteristics of the intentional defects after various chemical treatments, a pilot sample was fabricated. The sample has following characteristics: (1) the material of pilot sample comes from the same niobium piece which was used to fabricate this cavity; (2) the four pits on pilot sample have the same design parameters with the four pits in the cavity; (3) the mechanical or chemical treatments performed on the pilot sample is the same as the treatments applied to the cavity.

Geometrical Characterization of the 4 Pits Located on the Pilot Sample

3D shape analysis for the pits on pilot sample was performed by using a HIROX KH-7700 high resolution digital-video microscopy system (from college William &

Mary). Figure 3 shows the profile of the 4 pits.

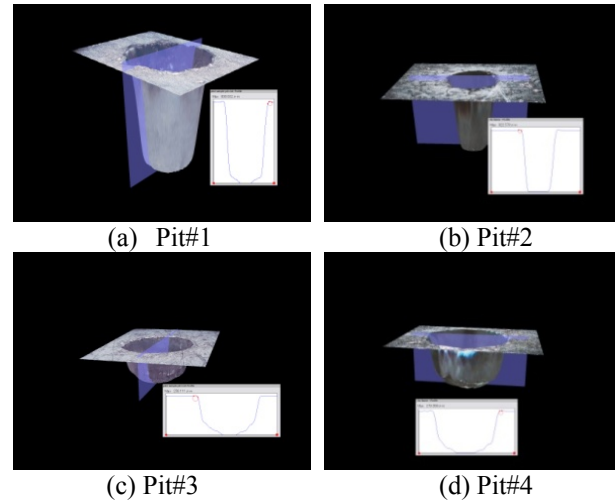


Figure 3: The geometrical profile of the 4 pits on pilot sample.

Once the defect profile is measured, the associated geometrical parameters and field enhancement factor for these four pits can be determined, as shown at Table 3.

Table 3: The geometrical parameters of 4 pits at pilot sample

Pit #	R/μm	L/μm	dz/mm	r/μm	β(≈)
1	485	835	5.5	22.9	2.7
2	550	820	9.0	24.3	2.7
3	460	256	6.8	18.7	2.7
4	470	280	9.5	13.9	3.2

It shows that the curvature radius of the four pits is between 10~25μm and the magnetic field enhancement factor is about 2.7~3.2. This result is at the range of our initial design: β≈3.

EDX for Foreign Material Detection

EDX (Energy-dispersive X-ray spectroscopy) was performed to detect is there any foreign material at the pilot sample. The data from pit #1 is shown in Figure 4; the data was qualitatively identical between all 4 pits. The results show that the foreign material includes carbon and oxygen at the pit area, which are commonly found on niobium surface. No other foreign material was detected by using EDX.

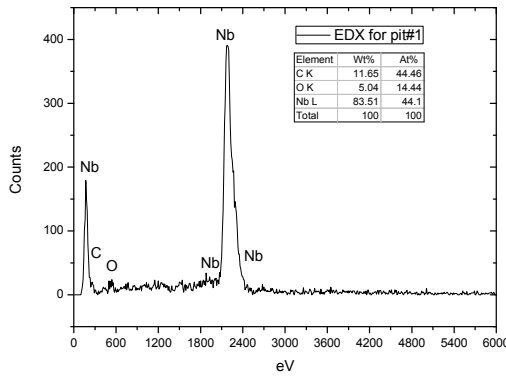


Figure 4: Foreign material analysis for pilot sample pit#1 (800µm depth) by EDX.

EXPERIMENTAL RESULTS

Then cold RF test for this cavity was performed at 2K. The cavity quenched at 12.7MV/m, as shown in Figure 5. There was an initial degradation in Q after the first quench, but the quenching field remained the same after quenches.

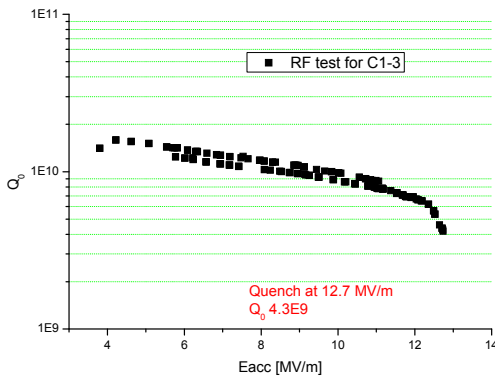


Figure 5: The RF test of CEBAF single cell cavity which has four intentional pit-type defects near the equator area.

During the RF test, the preheating behavior of this cavity was recorded by using the T-mapping system of Jefferson lab [8]. 576 temperature resistors are encased on the outer surface of this cavity to monitor the temperature behavior of the cavity. From Figure 6 we can see there is multiple preheating slopes transition in the thermometry data above some turn on field (6 MV/m) in the quenching defect: from 6 MV/m to 9 MV/m, from 9 MV/m to 12.3 MV/m, and finally from 12.3 MV/m to quench at 12.7 MV/m at 850mK. The other three defects seem to follow the same pattern as pit #1, although preheating starts at a higher field, and therefore does not reach the three zones before quench. The preheating data clearly suggest that there is a large difference between the 800 µm and 250 µm pits and in both cases the pits at 6mm have a higher preheating temperature than the pits at 9 mm. It is unclear why the difference in preheating between the 250 µm an

800 µm pits is so large; from the ANSYS data in Table 1 and 2, they should be approximately the same value.

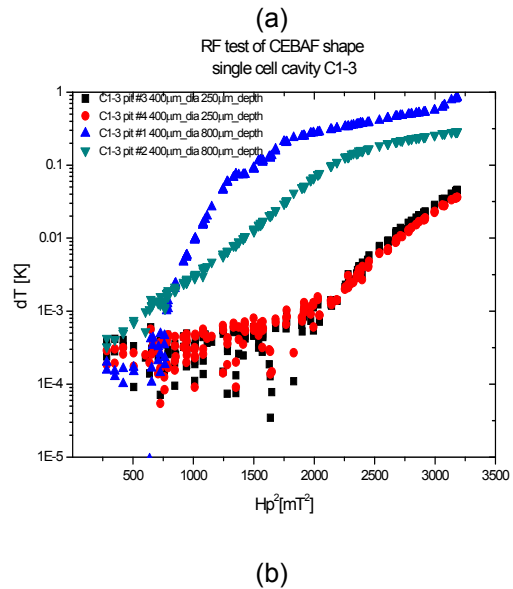
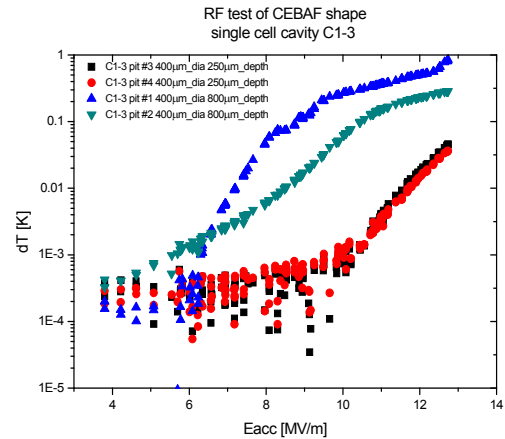


Figure 6: Preheating behavior of the CEBAF shape single cell cavity which was built with four intentional defects: (a) dT increases with Eacc; (b) dT increases with H_p^2 .

DISCUSSION AND CONCLUSIONS

Optical inspections of many 9-cell ILC cavities often reveal a topographical imperfection at the quench location; therefore we attempted to create a CEBAF-shaped cavity with artificial topographical features on the RF surface to explore magnetic enhancement role. Four pits with well-defined geometry were made on the cavity surface. Studies with pilot samples suggested that after pit creation and surface treatments the pits retained their modeled shape and were free of no foreign contamination which would skew the results.

Temperature measurements on these artificial defects during RF measurements show interesting behavior. First, as expected from numerical calculation, two shallow

pits with the smallest field enhancement factor have lowest temperature rise among four pits and did not cause the quench. Their preheating data as expected was very similar. Second, the two deep pits with the largest field enhancement factor showed stronger preheating. Third, the pit with the largest field enhancement factor and located closest to the equator caused quench in the cavity at the expected field level.

The temperature rise of the limiting defect shows several transitions to different slopes as the function of field, Figure 6. It is not clear if this result can be explained with a simple model of a single field enhancement feature on RF surface. We plan to do a numerical simulation of the pit-like defect on RF surface in order to understand observed preheating.

ACKNOWLEDGMENTS

The author would like to express thanks to Dr. Cheng for his support and helpful discussion during the course of this work. The author is also very thankful to all the group members of the applied research center of college William & Marry for their support of the HIROX equipment.

REFERENCES

- [1] R.A. Sherlock and D.O. Edwards, Oscillating Superleak Second Sound Transducers, Rev. Sci. Instrum. 41, Pg. 1603 (1970).
- [2] Mario Liu and Mario R. Stern, Oscillating Superleak Transducer of Second Sound, Physics review letters, Volume 48, Number 26, 28 June 1982.
- [3] Z. A. Conway, D. L. Hartill, H. S. Padamsee, and E. N. Smith, Oscillating superleak transducers for quench detection in superconducting ILC cavities cooled with HE-II, Proceedings of LINAC08, Victoria, BC, Canada.
- [4] K. Watanabe, Review of optical inspection methods and results, Proceedings of SRF, 2009, Berlin, Germany.
- [5] J. Dai, F. Furuta, K. Watanabe, R.L.Geng, K. Zhao, Optical observation of geometrical features and correlation with RF test results, this meeting.
- [6] K.Watanabe et al. Repair techniques of superconducting cavity for improvement cavity performance at KEK-STF, Proceedings of IPAC'10, Kyoto, Japan.
- [7] M Ge, G Wu, D Burk, J Ozelis, E Harms, D Sergatskov, D Hicks and L D Cooley, Routine characterization of 3D profiles of SRF cavity defects using replica techniques, Supercond. Sci. Technol. 24(2011)035002.
- [8] G. Ciovati, Jlab Technical note TN-05-59.